Rev. Roum. Sci. Techn.– Électrotechn. et Énerg.
Vol. **61**, *3*, pp. 258–262, Bucarest, 2016

ADAPTABLE SLIDING MODE CONTROL FOR WIND ENERGY APPLICATION

ADEL ABERBOUR, KASSA IDJDARENE, ZOUBIR BOUDRIES

Key words: Vector control, Sliding mode control, Chattering, Adaptable gains, Autonomous induction generator, Magnetic saturation.

This paper proposes an adaptable sliding mode control (A-SMC) scheme for an autonomous induction generator working with variable speed and load. The three-phase induction generator (IG) is excited using a PWM inverter connected to a single capacitor on the dc side. It is modelled through a diphase approach based on the application of the Park transform. The magnetic saturation phenomenon is included in the IG model. The control strategy should keep the dc voltage across the capacitor constant and equal to the reference value. The control takes a cascaded configuration, four SMCs in all. The outer control loops use adaptable gains and a tangent hyperbolic function, to ensure better performances in terms of response time, chattering and robustness. Finally, simulation results show the effectiveness of the proposed control strategy.

1. INTRODUCTION

As environmental pollution and climate change is increasingly evident, developing renewable energy sources has become the major subject of today's energy revolution, especially wind energy [1, 2]. Wind energy systems attracted the attention of researchers due to its non-polluting nature, abundance and relatively interesting cost.

The capability of the squirrel-cage induction generator, to excite without an external power supply, allowed its application in stand alone power generation systems. Furthermore, the squirrel-cage induction generator has many advantages over other types of electric generators such as robustness, less cost and maintenance free operation, which makes of it a perfect candidate for this type of operations.

Inductions generators are usually excited by three ac capacitors (capacitor bank) connected across its stator terminals and are known as self-excited induction generators (SEIGs). But, this method has some important drawbacks. The magnitude and frequency of the stator voltage are very sensitive to the variations of the rotation speed and the load value. Thus, this needs an appropriate voltage regulating scheme to maintain a constant voltage level regardless of load and/or speed, by controlling the reactive power transmitted to the generator [3]. To achieve this purpose, many schemes have been suggested. The widely used solution consists in connecting the stator windings of the induction generator directly to a rectifier/inverter system. In this case, the device must be controlled. To reach this goal, a direct torque control (DTC) is used [4]. This approach is quite effective and does not require an accurate knowledge of the machine model but it uses a hysteresis-band controller which increases the losses. In addition, as this approach is sensitive to the stator resistance value, the accuracy of the flux estimation can be reduced at low voltage. Another alternative to the DTC is vector control [3, 5]. Most of the SEIG vector control systems reported in literature use classical proportional integral (PI) controllers for voltage and/or flux control. Besides, PI-controller is very interesting due to its high mathematical accuracy but it is sensitive to the system parameter variations and can reject external disturbances inadequately. More advanced controllers, such as fuzzy logic control (FLC) [6] or sliding mode control (SMC) [7] have also been considered in SEIG control systems. It is reported that such controllers bring considerable performances in terms of response time, settling time and robustness.

In this paper, SMC based on vector control concepts is used to control an autonomous IG. Instead of the conventional PI controllers, the SMC is employed for each inner and outer control loops. The Lyapunov direct method is used to ensure the reaching and sustaining of the sliding mode. The control strategy takes a cascaded structure; the references of the current components are generated by the external SMCs, which use a hyperbolic tangent function instead of conventional sign function and adaptable gains instead of constant ones. So, the transient of the hitting control will be smoothed and the chattering phenomenon is alleviated without loosing the system robustness.

2. STUDIED SYSTEM

The studied system, shown in Fig 1, is constituted of a squirrel cage three-phase induction generator (IG) connected mechanically to a wind turbine through a gear box and electrically to a PWM rectifier/inverter. The dc side of the latter is connected to a capacitor, a battery to start up the system if no remnant voltage is available and a diode which decouples the battery from the rectifier/inverter as soon as the dc voltage generated is higher than the one of the battery. The load R is equivalent to the global load seen from the dc side. The block diagram of the control scheme is also shown on the same figure.

3. MATHEMATICAL MODEL OF THE INDUCTION MACHINE

Dynamic induction machine models are used as the basis for the design and implementation of control algorithms. Reliable and good control performance requires more detailed models. The parameters of the machine vary due to the variation of operating point, flux and frequency. At low flux values, the inductances remain constant, but as the flux increases, the machine starts to saturate and the inductances decrease. Hence, the accuracy of the model prediction and

Université de Bejaia, Faculté de Technologie, Laboratoire de Technologie Industrielle et de l'Information (LTII), 06000, Algérie, E-mail: aberbouradel@yahoo.fr, idjdarene@yahoo.fr, zboudries@yahoo.fr.

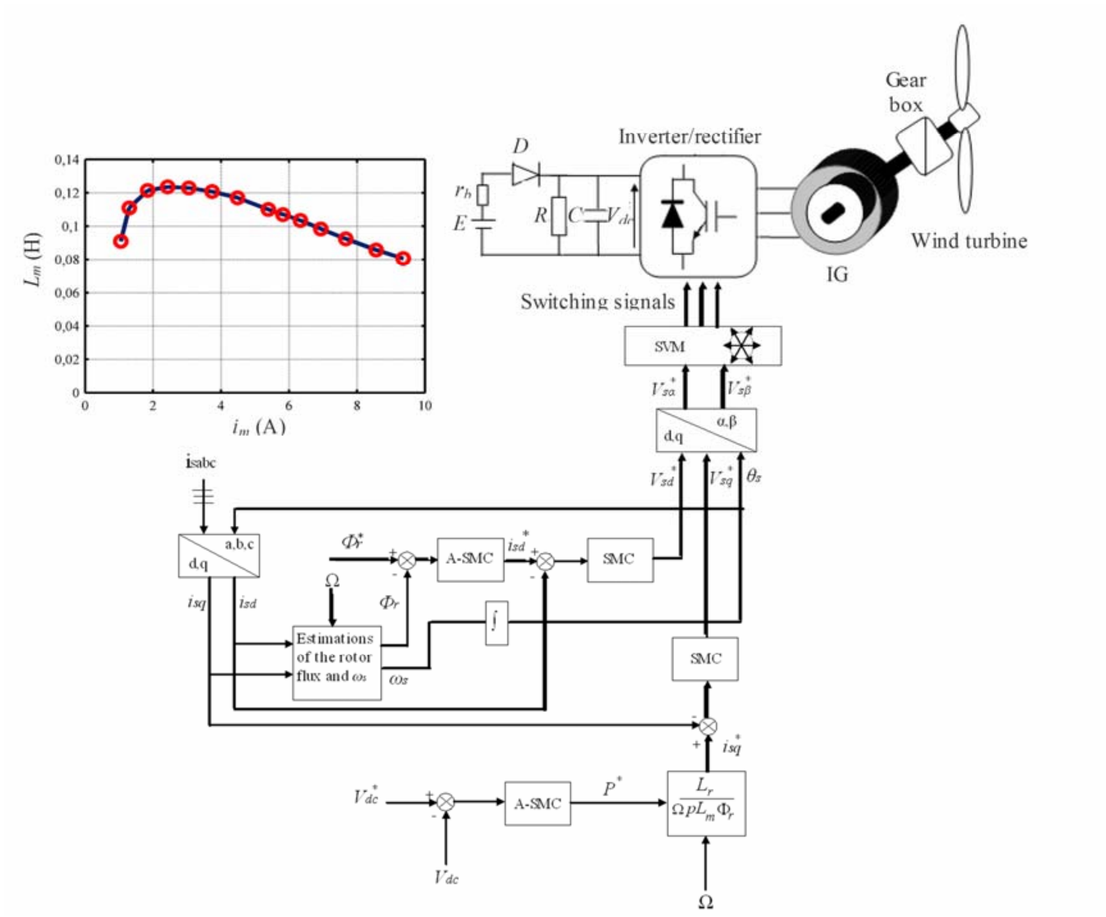

Fig. 1 – System and control scheme.

the control performance can be improved by including the magnetic saturation phenomenon into account. This is done via a variable magnetising inductance, through the estimation of the magnertising current.

The induction machine model can be written in the synchronous reference frame as follows [3]:

$$\begin{bmatrix} V_{sd} \\ V_{sq} \\ 0 \\ 0 \end{bmatrix} = \begin{bmatrix} R_s & -\omega_s . l_s & 0 & -\omega_s . L_m \\ \omega_s . l_s & R_s & \omega_s . L_m & 0 \\ -R_r & \omega_r \; . l_r & R_r & -\omega_r .(l_r + L_m) \\ -\omega_r \; . l_r & -R_r & \omega_r .(l_r + L_m) & R_r \end{bmatrix} \cdot \begin{bmatrix} i_{sd} \\ i_{sq} \\ i_{md} \\ i_{mq} \end{bmatrix} + \begin{bmatrix} l_s & 0 & L_m + L_m' \cdot \frac{i_{md}^2}{|i_m|} & L_m' \cdot \frac{i_{md} \cdot i_{mq}}{|i_m|} \\ 0 & l_s & L_m' \cdot \frac{i_{md} \cdot i_{mq}}{|i_m|} & L_m + L_m' \cdot \frac{i_{mq}^2}{|i_m|} \\ -l_r & 0 & l_r + L_m + L_m' \cdot \frac{i_{md}^2}{|i_m|} & L_m' \cdot \frac{i_{md} \cdot i_{mq}}{|i_m|} \\ 0 & -l_r & L_m' \cdot \frac{i_{md} \cdot i_{mq}}{|i_m|} & l_r + L_m + L_m' \cdot \frac{i_{mq}^2}{|i_m|} \end{bmatrix} \cdot \begin{bmatrix} \frac{di_{sd}}{dt} \\ \frac{di_{sq}}{dt} \\ \frac{di_{md}}{dt} \\ \frac{di_{mq}}{dt} \end{bmatrix}, \tag{1}$$

where R_s, l_s, R_r and l_r are the stator and rotor phase resistances and leakage inductances respectively, L_m and L_m' are the magnetising inductance and its derivative with respect to magnetising current and ω_s and ω_r are the stator and rotor electrical frequencies respectively. Besides, V_{sd}, i_{sd}, V_{sq} and i_{sq} are the d-q stator voltages and currents respectively. i_{md} and i_{mq} are the magnetising currents, along the d and q axis, given by:

$$\begin{cases} i_{md} = i_{sd} + i_{rd} \\ i_{mq} = i_{sq} + i_{rq} \end{cases} \quad \text{and} \quad i_m = \sqrt{i_{md}^2 + i_{mq}^2} \; . \tag{2}$$

To express L_m with respect to i_m, several approaches can be used, whose simplest one is the polynomial approximation.

$$L_m = f\left(\left|i_m\right|\right) = \sum_{j=0}^{n} a_j \cdot \left|i_m\right|^j \; . \tag{3}$$

The waveform of the magnetising inductance is obtained through tests at no load for different voltage magnitudes. In Fig. 1 above, we show a comparison between measurements and approximated values of a magnetising inductance L_m *versus* i_m.

4. CONTROL STRATEGY

Generally, in vector control algorithms the flux is kept constant at its rated value. Thus the torque can be adjusted according to the active power demand. In fact, as the flux is controlled to be constant, its variation around the operating points is negligible. Thus the inductances can also be considered constant ($L_{md} = L_{mq} = M = 0.10474$ H) [3]. Therefore, the model of the IG used for the control is simplified and can be considered as a linear one.

In the case of the present work, the orientation of the d-q frame is chosen such as $\Phi_{rd} = \Phi_r$ and $\Phi_{rq} = 0$. Therefore, the state equation of the stator currents can be re-written as:

$$\frac{di_{sd}}{dt}=\frac{1}{\sigma.L_s}\left(-R_s.i_{sd}+\omega_s.\sigma.L_s.i_{sq}-\frac{M}{L_r}.\frac{d\Phi_r}{dt}+V_{sd}\right), \tag{4}$$

$$\frac{di_{sq}}{dt}=\frac{1}{\sigma.L_s}\left(-R_s.i_{sq}-\omega_s.\sigma.L_s.i_{sd}-\omega_s.\frac{M}{L_r}.\Phi_r+V_{sq}\right), \tag{5}$$

where: $\sigma=1-M^2/(L_sL_r)$, is the leakage flux coefficient. $L_s=l_s+M$ and $L_r=l_r+M$, are the stator and rotor self inductances.

The rotor flux, electromagnetic torque and the synchronous frequency can be estimated as follows [3]:

$$\Phi_r=\frac{Mi_{sd}}{1+\tau_r s},\qquad T_{em}=p\frac{M}{L_r}\Phi_r i_{sq}\ \text{ and }\ \omega_s=\frac{Mi_{sq}}{\tau_r\Phi_r}+p\Omega, \tag{6}$$

where s is the time derivative operator, $\tau_r=L_r/R_r$ is rotor time constant, Ω is the mechanical speed of the machine which is measured continuously and p is the pole pair number.

4.1. SLIDING MODE CONTROL DESIGN

According to the sliding mode theory, the first designing step consists in defining the switching functions (sliding surfaces). In the case of this paper, four sliding surfaces related to control objectives are defined as follows:

$$\begin{cases} S(i_{sd})=i_{sd}^*-i_{sd}, \\ S(i_{sq})=i_{sq}^*-i_{sq}, \\ S(V_{dc})=V_{dc}^*-V_{dc}, \\ S(\Phi_r)=\Phi_r^*-\Phi_r. \end{cases} \tag{7}$$

The sufficiency conditions for the existence and sustaining of the sliding mode is given as follows:

$$\frac{dS(x)}{dt}\operatorname{sign}(S(x))\le-\eta, \tag{8}$$

with η is a positive constant. If we keep different signs for the sliding surface and its derivative, the controlled variable will be attracted toward it, which means the existence of a sliding motion on the sliding surface $S(x)$. In other words, the verification of the condition (8) implies stability of the system.

In the following, we will design the corresponding control law for each sliding surface.

4.1.1. SLIDING MODE CURRENTS CONTROL DESIGN (INTERNAL LOOP)

The sliding mode control laws of the d and q-axis current components are given as follows:

$$V_{sd}^*=\left(\left(R_s.i_{sd}-\omega_s.\sigma.L_s.i_{sq}+\frac{M}{L_r}\cdot\frac{d\Phi_r}{dt}\right)+\sigma.L_s.\frac{di_{sd}^*}{dt}\right)+ \\ +K_d.\operatorname{sign}\left(S\left(i_{sd}\right)\right), \tag{9}$$

$$V_{sq}^*=\left(\left(R_s.i_{sq}+\omega_s.\sigma.L_s.i_{sd}+\omega_s.\frac{M}{L_r}\cdot\Phi_r\right)+\sigma.L_s.\frac{di_{sq}^*}{dt}\right)+ \\ +K_q.\operatorname{sign}\left(S\left(i_{sq}\right)\right). \tag{10}$$

As it can be seen from (9) and (10), there are two terms in the control law, a continuous and a discontinuous one. The continuous term reflects knowledge of the system dynamics, it is the so-called equivalent control, whose main rule is to maintain the controlled variable on the sliding surface but it is not intended to attract it towards it. This task is devoted to the discontinuous control action, which ensures the sliding to occur. However, this controller leads to limited performance due to the high control activity resulting in chattering. To reduce the latter, we will introduce a hyperbolic tangent function instead of sign function. It results in a smooth control signal. Then, the control laws (9) and (10) become:

$$V_{sd}^*=\left(\left(R_s.i_{sd}-\omega_s.\sigma.L_s.i_{sq}+\frac{M}{L_r}\cdot\frac{d\Phi_r}{dt}\right)+\sigma.L_s.\frac{di_{sd}^*}{dt}\right)+ \\ +K_d.\tanh\left(\frac{S(i_{sd})}{\varepsilon}\right), \tag{11}$$

$$V_{sq}^*=\left(\left(R_s.i_{sq}+\omega_s.\sigma.L_s.i_{sd}+\omega_s.\frac{M}{L_r}\cdot\Phi_r\right)+\sigma.L_s.\frac{di_{sq}^*}{dt}\right)+ \\ +K_q.\tanh\left(\frac{S(i_{sq})}{\varepsilon}\right), \tag{12}$$

where ε defines the thickness of the boundary layer.

4.1.2. ROTOR FLUX AND DC-VOLTAGE SLIDING MODE CONTROL DESIGN (EXTERNAL LOOP)

The rotor flux and the dc voltage state equations are given as follow:

$$\begin{cases} \dfrac{d\Phi_r}{dt}=\dfrac{M}{\tau_r}i_{sd}-\dfrac{1}{\tau_r}\Phi_r \\ \dfrac{dV_{dc}}{dt}=-\dfrac{i_L}{C}+\dfrac{i_{dc}}{C}=-\dfrac{V_{dc}}{R.C}+\dfrac{i_{dc}}{C} \end{cases}, \tag{13}$$

where C is the dc link capacitance and R is the resistive load. Besides, i_L and i_{dc} are the load current and the dc current respectively.

The SMC law of the rotor flux is given as:

$$i_{sd}^*=K_\Phi\tanh\left(\frac{S(\Phi_r)}{\varepsilon}\right)+\frac{\tau_r}{M}\left(\frac{d\Phi_r^*}{dt}+\frac{\Phi_r}{\tau_r}\right). \tag{14}$$

By assuming the following:

$$P_{dc}=V_{dc}.i_{dc}=T_{em}.\Omega. \tag{15}$$

Therefore, the SMC law of the dc voltage control loop is obtained:

$$i_{sq}^*=\frac{L_r.V_{dc}}{p.\Omega.M.\Phi_r}\left(K_V.\tanh\left(\frac{S(V_{dc})}{\varepsilon}\right)+i_L\right). \tag{16}$$

The gains of the outer control loops are self-adjustable for performance improvement and are given as follows:

$$K_\Phi=\lambda_\Phi\left|S(\Phi_r)\right|^\alpha,\quad K_V=\lambda_V\left|S(V_{dc})\right|^\alpha \\ \text{with}\quad 0\le\alpha\le1, \tag{17}$$

where: λ_i ($i=\Phi$, V) is a positive integer. Note that the fact of using a sign function in the outer loop will lead to a harmful chattering, mainly due to the cascaded configuration of the controller; the output signals of the external loop are inputs of the internal loop. These signals will switch from a given maximal value to a minimal one. Hence, the waveforms of the stator currents will be affected and completely distorted. However, in the case of the present work, the problem of chattering is largely alleviated, thanks to the adaptable gain and to the hyperbolic tangent function which smoothes the transient of the hitting control without loosing the system robustness while keeping a good behaviour of the stator currents.

5. SIMULATION RESULTS

The logic control signals of the PWM converter are calculated by using the space vector modulation (SVM) technique. The details about its implementation can be found in [8]. The model of the induction generator used in this simulation is the one given in equation (1) which takes the saturation effect into account.

The nominal parameters of the induction machine are listed in the appendix. The dc voltage reference value is put equal to $V_{dc}^* = 600$ V. The reference rotor flux is put equal to the rated value $\Phi_r^* = 0.7$ Wb. The value of the load resistance R is initially equal to 70 Ω which is the value that allows the machine to generate a significant power related to the operating conditions. At $t = 2$ s the resistance is increased to $R = 140$ Ω, then it is decreased to its initial value at $t = 4$ s. For this test, an accelerated random rotor speed with wide range of variation is imposed, its waveform around the synchronous value (Ω = 750 rpm) is given in Fig. 2.

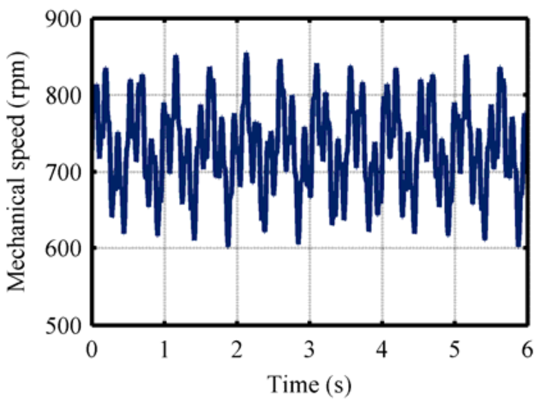

Fig. 2 – Rotor speed.

Note that the rotor speed time waveform which is imposed (Fig. 2) is not encountered in real wind power conversion systems due to the limited dynamics of commonly used prime movers. The speed disturbances are intentionally exaggerated to highlight the advantage of the developed control strategy over the conventional used PI controllers in terms of robustness to speed variations. The parameters of the PI controllers are chosen optimally by observing the behaviour of the controlled variables for different combinations of the proportional and the integral gains, based on the criteria of fast response, small overshoot and robustness.

Figures 3 and 4 show that, the proposed control strategy (Fig. 3) exhibits more robust response to the imposed speed and load disturbances compared to the PI controller (Fig. 4). More specifically, in the case of the latter, the speed disturbance induces dc voltage ripples while the proposed strategy manages to eliminate them. It can be observed that the response of the dc voltage obtained by the SMC is insensitive to the applied step change in the load resistance. Concerning the strategy with PI controllers, we can observe an overshoot of about 10% caused by increasing the resistance value at $t = 2$ s and an undershoot with almost the same magnitude due to the restoration of the load resistance to its initial value at $t = 4$ s. The obtained results confirm the advantages of the studied control strategy over the usually used PI controllers in terms of robustness against load and speed disturbances. For both cases (Figs. 5 and 6), the rotor flux is well controlled and established to a constant value, with faster response concerning the SMC controller (Fig. 5).

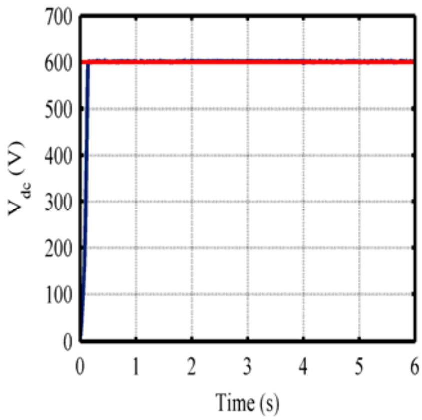

Fig. 3 – Dc voltage – SMC method.

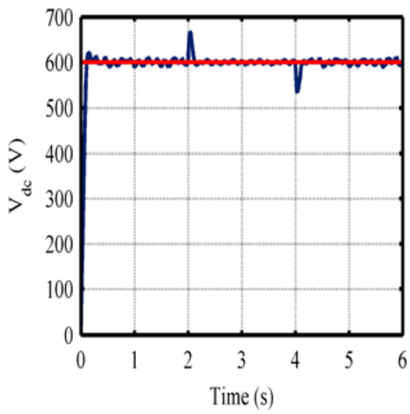

Fig. 4 – Dc voltage – PI controller.

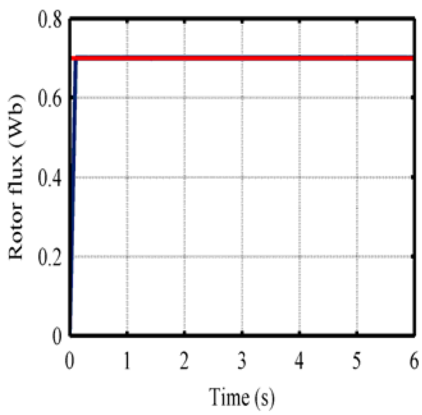

Fig. 5 – Rotor flux – SMC method.

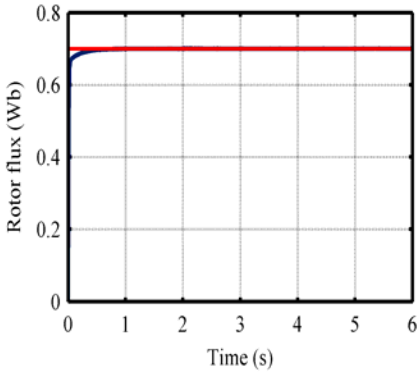

Fig. 6 – Rotor flux – PI controller.

As can be observed on the behaviour of the q-axis stator current component as well as the zooms of stator currents (Fig. 7), the proposed strategy exhibits high dynamic transition when the step changes in the load resistance occur, then permits to compensate quickly these disturbances. Thus, the dc voltage is not affected as confirmed in Fig. 3. On the other side, the obtained q-axis stator current component with PI controller (Fig. 8) has a low dynamic transition when the load resistance is varied. Hence, the perturbation is not compensated adequately, as confirmed in Fig. 4.

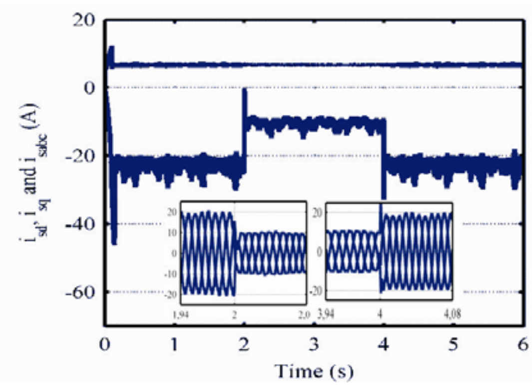

Fig. 7 – Stator currents – SMC method.

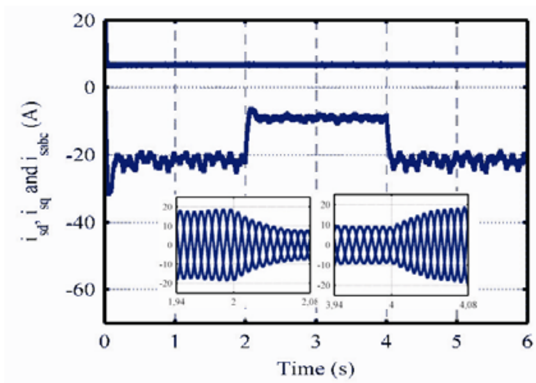

Fig. 8 – Stator currents – PI controller.

6. CONCLUSION

In this paper, vector control with an A-SMC and SMC of an induction generator used in an autonomous variable speed wind system is studied. An analytical model of the autonomous induction generator, taking the saturation effects into account, by the means of a variable magnetising inductance, has been presented. The control leads us to feed the load with voltage of constant effective value, whatever the speed of the turbine and the load. The simulation results show that the proposed control scheme has high performance dynamic characteristics and shows very strong robustness compared to the usually used PI controller. The chattering problem encountered in SMC is largely alleviated without loosing the system robustness, thanks to the adaptable gains and to the hyperbolic tangent function. Simple and robust, the proposed method is quite relevant for an isolated wind energy conversion system based on a squirrel cage induction generator.

APPENDIX

Parameters of the induction machine:
$P_N = 5.5$ kW, $U_N = 230/400$ V, $I_N = 23.8/13.7$ A, 50 Hz, $\Omega_N = 690$ rpm, $J = 0.230$ kg·m^2, $d = 0.0025$ N·m/rads^{-1}, R_s= 1.07131 Ω, R_r= 1.29511 Ω, $p = 4$.

Received on September 5, 2015

REFERENCES

1. M. Adjoudj, M. Abid, A. Aissaoui, Y. Ramdani, H. Bounoua, *Sliding mode control of a doubly fed induction generator for wind turbines*, Rev. Roum. Sci. Techn. – Électrotechn. et Énerg., **56**, *1*, pp. 15–24 (2011).
2. M. Doumi, A. Aissaoui, A. Tahour, M. Abid, *Commande adaptative d'un système éolien*, Rev. Roum. Sci. Techn. – Électrotechn. et Énerg., **60**, *1*, pp. 99–110 (2015).
3. K. Idjdarene, D. Rekioua, T. Rekioua, A. Tounzi, *Vector control of autonomous induction generator taking saturation effect into account*, Energy Conversion and Management, **49**, pp. 2609–2617 (2008).
4. S. Hammadi, N. Hidouri, L. Sbita, *A DTC SEIG drive scheme for an isolated wind turbine buck system*, International Conference on Control, Decision and Information Technologies (CoDIT'13), pp. 543–548 (2013).
5. E. Levi, Y.W. Liao, *Rotor flux oriented induction machine as a DC power generator*, The 8th European Conference on Power Electronics and Applications (EPE'99), pp. 1–8 (1999).
6. M. Bašić, D. Vukadinović, M. Polić, *Fuzzy DC-voltage controller for a vector controlled stand-alone induction generator*, International Journal of Circuits, Systems and Signal Processing, **7**, *3*, pp. 181–190 (2013).
7. L. Louze, A.L. Memmour, A. Khezzar, M. Boucherma, *Input-output linearizing and sliding mode control schemes for a self-excited induction generator*, 35th Annual Conference of IEEE Industrial Electronics (IECON'09), pp. 3892–3897 (2009).
8. T.J. Fu, W.F. Xie, *A novel sliding-mode control of induction motor using space vector modulation technique*, ISA transactions, **44**, pp. 481–490 (2005).